

Anomalous Adsorption of Polyelectrolyte Layers

Stella Y. Park, Christopher J. Barrett,[†] Michael F. Rubner, and Anne M. Mayes*

Department of Materials Science and Engineering and Center for Materials Science and Engineering, Massachusetts Institute of Technology, Cambridge, Massachusetts 02139

Received September 14, 2000; Revised Manuscript Received February 14, 2001

ABSTRACT: We study the adsorption of polyelectrolytes onto oppositely charged surfaces as the surface charge density is varied while keeping the polyelectrolyte charge density fixed. As observed previously from multilayer adsorption studies,^{1,2} nonmonotonic adsorption behavior is obtained in the intermediate surface charge density regime, with anomalously thick “supermonolayers” transitioning to molecularly thin layers over a small range of surface charge densities. A simple adsorption model is introduced to explain these findings, in which the surface is characterized by discrete and fully compensated adsorption sites.

1. Introduction

The adsorption of charged polymers, or polyelectrolytes, onto oppositely charged surfaces from aqueous solutions is an underlying phenomenon for a wide range of industrially and biologically significant processes, such as cell adhesion, viral infection, and wastewater treatment.^{3–5} The layering of polyelectrolytes onto charged surfaces has also received strong interest as a novel processing technique for assembly of thin film coatings and multilayer electrooptic devices.^{6–8} Although thick adsorbed layers are desirable for many of these applications, most studies to date have involved systems that adsorb as molecularly thin layers.

Recent multilayer deposition studies of nearly completely ionized (dissociation fraction $\alpha \approx 0.7–0.9$) polyelectrolytes indicate adsorption of unusually thick layers.^{1,2} For example, layers of poly(acrylic acid) (PAA, $pK_a \approx 5.0$) and poly(allylamine) (PAH, $pK_b \approx 10.5$) with average dried layer thicknesses in excess of 80 Å have been observed; this is an order of magnitude above what is typically seen when fully charged polyelectrolytes are deposited onto surfaces in the absence of added salt. In fact, when PAA and PAH are sequentially adsorbed as fully charged polyelectrolytes, the average dried layer thickness is only ≈ 2.5 Å. This transition from deposition of very thick layers to molecularly thin layers occurs with a remarkably small change in pH. Behavior of this type has not been predicted by any of the previous models of polyelectrolyte adsorption,^{9–21} and hence represents a fundamentally different adsorption regime.

Theoretical treatments of adsorption of polymers to surfaces have mainly considered surfaces on which the charge is continuously and uniformly distributed. Using the self-consistent mean-field (SCF) theories developed by Scheutjens and Fleer,¹¹ adsorption of weak⁹ and strong polyelectrolytes¹⁸ onto these surfaces were modeled, incorporating the electrostatic models of Muthukumar,¹⁰ with later refinements by Israëls.¹² SCF models have been further developed to incorporate variable surface charge density in addition to variable charge on the chain.^{13,14,16} In such mean-field treatments, surface charges are smeared out, rather than

discrete. Heterogeneity of adsorbing surfaces^{21–23} has also been studied to investigate the effect of having a nonuniform distribution of adsorbing sites. While these models qualitatively capture many aspects of polyelectrolyte adsorption, they nonetheless fail to predict the tens-of-angstroms thick “supermonolayers” observed in recent multilayer deposition studies.^{1,2} As discussed below, this adsorption behavior can also be observed using charge-regulated self-assembled monolayer (SAM) surfaces (see Figure 1).

In this paper, we hypothesize that this anomalous adsorption behavior arises from the discrete nature of the surface charges. For purposes of modeling this physical system, the adsorption may be more accurately described as anchoring a monomer site onto a matching discrete (“sticker”) site on the surface which has an average dimensionless sticker density σ . In the extreme regimes of surface sticker density (very high or very low), the adsorption behavior is essentially the same as that predicted by earlier models.^{13,14,16,17} However, when the average distance between stickers lies between that of the segment size and the adsorbing chain dimension, supermonolayers can be deposited.

Here we briefly present first the adsorption results obtained using charge-regulated SAMs to demonstrate that supermonolayer deposition and the transition to molecularly thin layers observed in recent multilayer studies^{1,2} are, to a great extent, governed by the surface charge density. We then outline a simple free energy model for polyelectrolyte adsorption that incorporates discrete sticker sites, and qualitatively captures these results.

2. Experimental Results

Self-assembled monolayer (SAM) charge-regulated surfaces were prepared on cleaned Si wafers by treating with 3-aminopropyltrimethoxysilane, similar to previously reported treatments.^{25,26} The resulting amine surfaces were then immersed for 20 min into one of 15 solutions of 10^{-2} M 90 000 g/mol PAA fixed to a pH value between 9.0 and 12.5 using HCl. With a pK_a of ≈ 10.5 , the fraction of protonated surface amino groups is expected to range from 0.98 to 0.01, corresponding to a charge density range of $4–0.04$ nm⁻².²⁶ Note that PAA is fully charged over this pH range. The samples were rinsed with deionized water and dried first under a gentle stream of N₂ and then in an 80 °C oven for 2 h. The thickness of the total organic layer (SAM + PAA) was measured by ellipsometry.

* Corresponding author.

[†] Present address: Department of Chemistry, McGill University, Montreal, Canada.

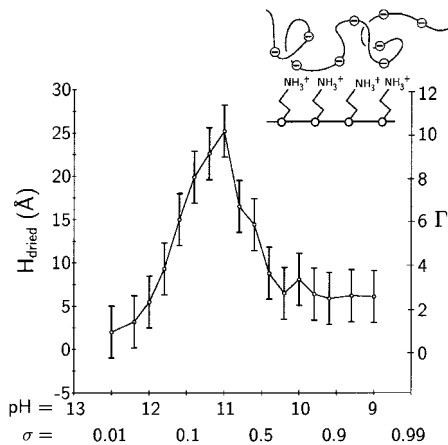


Figure 1. Dried PAA layer thickness H_{dried} and dimensionless adsorbed amount Γ on SAM as a function of pH (dimensionless surface charge density σ) with schematic of the positively charged surface.

The average thickness of the SAM was measured independently to be 6.5 Å. This value was subtracted from the total layer height to obtain the PAA dried layer thickness shown in Figure 1. The dried layer thickness H_{dried} and the dimensionless PAA adsorbed amount Γ are plotted as a function of the charge density σ and the solution pH. The dimensionless adsorbed amount is defined as $\Gamma \equiv \phi H/a = H_{\text{dried}}/a$ where H and ϕ are the hydrated layer height and polymer volume fraction, respectively, and a the segment length ≈ 2.5 Å.

It is clear from Figure 1 that a maximum adsorbed layer thickness ≈ 25 Å is deposited at a moderate charge density of 0.1–0.2/ a^2 , while at a greater charge fraction, a molecularly thin layer ($\Gamma \approx 2$) of polyelectrolyte is adsorbed. It is also clear from Figure 1 that the transition from thick deposition to monolayer coverage is a sharp one, with the adsorbed layer thickness falling from 25 to 5 Å over a narrow pH range between 11.0 and 10.5. This effect is also seen with added salt ($\approx 10^{-2}$ M NaCl), providing further evidence that this observation is predominantly a pH effect (and hence a surface charge variation effect) rather than an effect due to charge screening. Although the values seen here are less dramatic than in multilayer systems,^{1,2} the observation of both the excessive adsorbed amount (supermonolayer) and the sharp transition over a narrow pH range suggests that this behavior can be regarded in large part as a surface effect, depending strongly on the surface charge density.

Our next aim is to describe the adsorption through a simple free energy model that incorporates *site-specific adsorption* through sticker interactions. The excluded volume and entropy terms are similar to those frequently employed for weakly charged or neutral chain adsorption.^{27–32} Heretofore, all free energies are expressed per chain.

3. Adsorption Free Energy

We consider N -segment chains adsorbed onto a surface with sticker site density σ/a^2 . The bulk concentration of salt (counterions) is set equal to the experimental concentration of monomer units in solution ($\approx 10^{-2}$ M). Each chain segment corresponds to a sticker site, the linear density of sticker sites being equivalent to that of a fully charged chain. Each chain in the adsorbed layer can be defined by its adsorbed height in solution H and lateral dimension R . The number of anchored segments (or loops) per chain, N/n where n is the loop length between sticking sites,²⁴ follows the relationship $(N/n) = \sigma(R^2/a^2)$. The segment volume fraction ϕ is assumed to be uniform throughout the layer and is given by $\phi \approx (Na^3/R^2H)$ so that $(N/n) \approx (\sigma Na/\phi H)$. The adsorption free energy is written

$$F_{\text{ad}} = F_{\text{conf}} + F_{\text{stick}} + F_{\text{rep}} \quad (1)$$

where conf, stick, and rep subscripts correspond to conformational, sticker, and segment–segment repulsive free energies, respectively.

3.1. Conformational Entropy. The conformational entropy penalty for adsorption can be separated into two parts, a coil deformation term, F_{elas} , and a second term F_{loop} arising from the localization of the required number of segments at the surface sticker sites:

$$F_{\text{conf}} = F_{\text{elas}} + F_{\text{loop}} \quad (2)$$

The elastic term is written as the usual penalty for stretching or compressing a Gaussian coil

$$\begin{aligned} \beta F_{\text{elas}} &= \beta F_{\text{comp}} + \beta F_{\text{elong}} \\ &\approx \frac{3}{2} \left(\frac{R_0^2}{H^2} - 1 \right) + \frac{3}{2} \left(\frac{H^2}{R_0^2} - 1 \right) \end{aligned} \quad (3)$$

where $\beta = 1/k_B T$ and R_0 is the ideal coil size, i.e., $R_0^2 \approx Na^2$. Because of the discrete nature of the stickers, an additional loss of conformational entropy arises by tacking down N/n segments to surface sticker sites. This term corresponds to the *excess* loss of conformation of a chain upon confinement of a monomer per loop, of which there are N/n per chain, to a sticker site. This can be considered simplistically by using a lattice approach (see Appendix A) and can be approximated

$$\beta F_{\text{loop}} \approx \frac{N}{n} \ln \left(\frac{H}{\sigma a} \right) - \frac{(1-\phi)}{\phi} \frac{N}{n} \ln(1-\phi) \quad (4)$$

Considering just the first term, it is clear that this is the entropic cost of confining N/n segments, initially distributed within layer height H , to sticker sites in the layer adjacent to the surface. As σ increases, this entropic penalty increases.

3.2. “Sticker” Energy. If the attractive potential between the charged group on the polyelectrolyte and the charged surface (discrete sticker) group is sufficiently short-ranged, i.e., the two oppositely charged groups form a “salt” (or sticker pair) with zero net charge, then we can assume an adsorption energy

$$\begin{aligned} \beta F_{\text{stick}} &\approx -\delta \frac{N}{n} \\ &\approx -\delta \frac{\sigma Na}{\phi H} \end{aligned} \quad (5)$$

where $\delta k_B T$ is an energy per salt pair (or sticker pair) formation. Note that implicit in the derivation of eqs 4 and 5 is the requirement that *all stickers sites be paired*.

3.3. Segment–Segment Repulsions. We consider two possible types of segment–segment repulsions: (1) excluded volume and (2) electrostatic. The excluded volume interaction per molecule is²⁹

$$\beta F_{\text{vol}} \approx \left(\frac{1}{2} - \chi \right) N \phi \quad (6)$$

which becomes

$$\beta F_{\text{vol}} \approx \frac{1}{2} N \phi \quad (7)$$

for $\chi = 0$ (athermal solvent). In the case of electrostatic

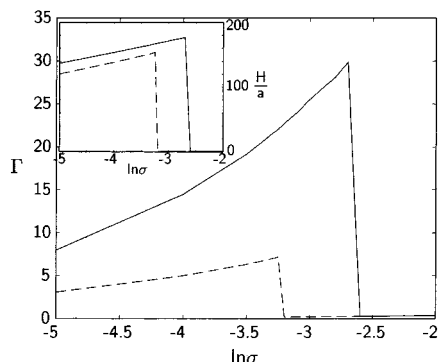


Figure 2. $\Gamma(\equiv\phi H/a)$ for $\delta = 5$, $N = 2000$ as a function of surface sticker density σ : (—) using F_{elec} ; (---) using F_{vol} . The inset shows the change in hydrated layer height H/a with σ .

segment–segment repulsions per chain for a fully charged polyelectrolyte, we can borrow from Netz and Joanny's derivation¹⁵ of the layer self-energy

$$\beta F_{\text{elec}} = \frac{\pi N l_B \phi}{\kappa^3 H^3 a} (e^{-2\kappa H} - 1 + 2\kappa H) \quad (8)$$

where l_B is the Bjerrum length (≈ 7 Å for water at room temperature), κ is the Debye parameter (here, in the absence of salt, proportional to the square root of the monomer concentration, i.e., $\kappa^{-1} \approx 30$ Å), and e is the unit charge.

4. Adsorption Transition

The total adsorption free energy, F_{ad} (sum of eqs 3–5, and 7 or 8) must be minimized with respect to ϕ and H to find the equilibrium adsorbed amount Γ for any σ and δ (see Appendix B). The adsorption profile Γ for $\delta = 5$ and $N = 2000$ is plotted vs σ in Figure 2. Focusing first on the region of the plot where $\ln \sigma < -2.6$, the model appears to qualitatively capture the dramatic “supermonolayer” growth observed experimentally for intermediate surface charge densities. The increase in adsorbed mass with increasing sticker density reflects an increase in both the hydrated layer concentration (ϕ) and height (H), as can be deduced from the inset in Figure 2. For example, assuming electrostatic self-interactions (solid lines), the hydrated layer concentration rises from $\phi \approx 0.06$ for $\sigma \approx 0.007$ to $\phi \approx 0.17$ for $\sigma \approx 0.067$.

With increasing surface charge density, the value of F_{ad} computed from the minimization of eq 1 increases. Comparing F_{ad} to the reference free energy for a molecularly thin adsorbed monolayer, $F_{\text{ref}} = F_{\text{ad}}(\phi_{\text{thin}}, H = a)$ where $\phi_{\text{thin}} = \sigma^{1/2}$, a transition to molecularly thin layers is predicted for intermediate surface charge densities, similar to that seen experimentally in Figure 1.

Figure 2 demonstrates that the qualitative results obtained using either of the segment–segment repulsive terms—eq 7 or 8 (excluded volume or electrostatic self-energy)—are essentially the same, although the exact magnitudes differ. Indeed, such differences may be an artifact of the overestimate of segment–segment repulsions using eq 7 and the underestimate using eq 8. Hence, it should be the qualitative adsorption behavior and the order of magnitude agreement with the experimental Γ values and σ range of the transition (see Figure 1) that are emphasized here. The nature of the segment–segment repulsions, therefore, may be crucial

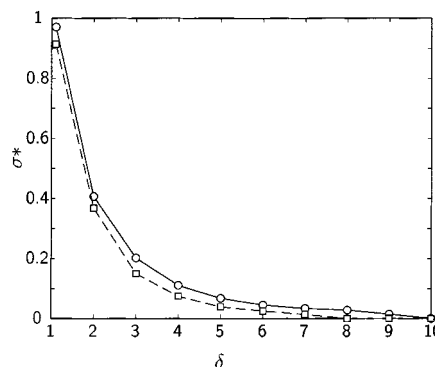


Figure 3. Transition sticker density σ^* as a function of δ for $N = 2000$ (○) using F_{elec} ; (□) using F_{vol} .

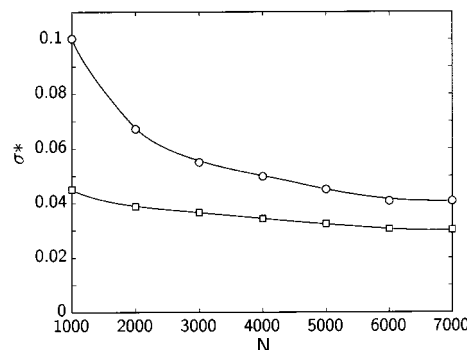


Figure 4. Change in σ^* as a function of chain length N : (○) using F_{elec} ; (□) using F_{vol} .

for determining the transition point and the total adsorbed amount, but *not* the general adsorption behavior. It is rather F_{loop} that is responsible for the transition, i.e., the description of the adsorption site as discrete, rather than smeared out, and the requirement that *all* surface sites be paired, that changes the nature of coverage and adsorption.

Furthermore, a transition diagram can be plotted to show the transition sticker density σ^* as a function of the phenomenological sticker energy δ (see Figure 3). If $\delta \leq 1$, there is no solution to the minimization; i.e., the entropic cost of adsorption outweighs the enthalpic gain. If $\delta \geq 10$, only molecularly thin layers are observed, i.e., $F_{\text{ad}} > F_{\text{ref}}$ is always true. However, if $1 < \delta < 10$, we observe the transition from “supermonolayer” to “monolayer” coverage, giving evidence to tunable layer height with small changes in the surface charge density. It is interesting to note that previous estimates of electrostatic sticking energy³⁵ fall within the δ range predicted to give rise to anomalous adsorption behavior.

To understand how this transition varies with chain length, the transition sticker density σ^* as a function of N is plotted in Figure 4 for both types of segment–segment repulsion when $\delta = 5$. As expected, σ^* decreases with increasing N , becoming diminishingly dependent on chain length for $N \geq 2000$. This trend in σ^* reflects the decreasing dependence of F_{loop} on N with increasing chain length.

The hydrated layer height and the adsorbed amount at the transition also vary as functions of both δ and N and are plotted in Figure 5. The decrease in both Γ and H with increasing δ follows from the lower values of σ^* as shown in Figure 3. For high values of δ , the sticker energy dominates the free energy expression, and the enthalpic gain per chain becomes the driving force for

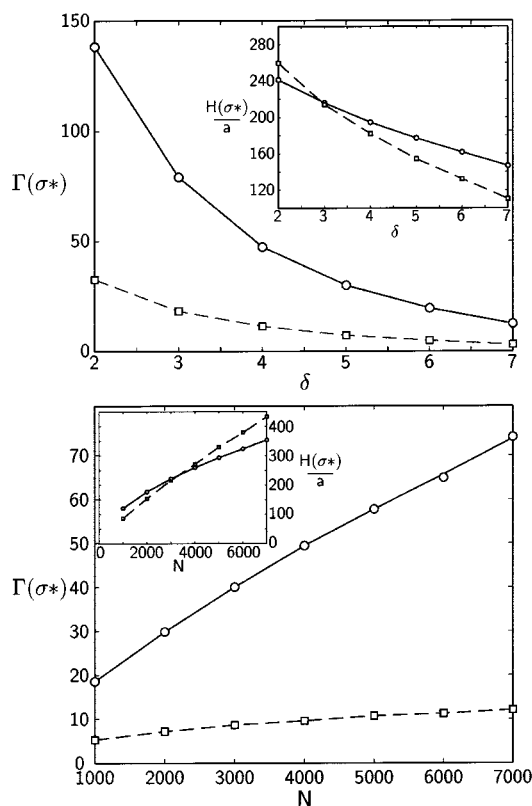


Figure 5. Adsorbed amount at transition for various values of δ (top) and N (bottom): $-\circ-$ using F_{elec} ; $(-\square-)$ using F_{vol} . Corresponding layer heights at the transition $H(\sigma^*)/a$ are shown in the insets.

monolayer deposition at lower values of σ . Though σ^* also decreases with increasing N , the simultaneous increase in $H(\sigma^*)$ leads to greater total adsorption amounts.

5. Discussion

Results in section 2 demonstrate that the thickness of adsorbed polyelectrolyte layers can vary markedly depending upon the fraction of attractive surface sites, with the greatest layer thicknesses observed for surfaces of intermediate charge fraction. Apparently, such “supermonolayer” adsorption processes^{1,2} can be accounted for through a molecular adsorption model that considers the spatially discrete nature of surface charges, while requiring that each surface sticker site be compensated for. Both of these aspects of the model appear important and both contrast with previous approaches, such as those employing numerical self-consistent field methods. For example, earlier works examining polyelectrolyte adsorption as a function of surface charge density^{9,18} typically consider a “smeared” surface charge, and predict a monotonically increasing surface coverage to roughly monolayer values at high surface charge densities. Other models that treat polymer adsorption onto heterogeneous surfaces—which comprise adsorbing and nonadsorbing discrete sites—predict similar submonolayer adsorption profiles as the fraction of adsorbing surface sites increases.²² All of these models employ the classical picture of Langmuir adsorption equilibrium with a probabilistic treatment of surface site occupation.

As it appears to have a significant bearing on our model predictions, some discussion is warranted on the assumption of full surface site occupancy. While adsorp-

tion of small molecules and surfactants is generally well characterized by the Langmuir adsorption model, adsorption of macromolecules differs fundamentally in its often irreversible nature. This can be explained as a consequence of the large energetic barrier—which may be orders of magnitude larger than $k_B T$ for chains anchored by many adsorbing segments—to removing a single coil from the surface. From another perspective, the adsorbed coil can be seen as creating a higher *effective* polymer concentration in the near-surface region, a concentration that is orders of magnitude higher than the surrounding solution. This *local* segment concentration (ϕ) adjacent to the surface dictates near-complete site occupancy.

Here, to physically understand the observed adsorption profile, we have oversimplified the adsorption such that the concentration profile of the adsorbed layer is a step function, i.e., the volume fraction ϕ is constant throughout the layer, and the undeformed size of the polyelectrolyte coil is essentially that of an ideal (uncharged) chain. We present a *qualitative* result, stressing that this phenomenon can be general to any polymer adsorption in which the adsorption energy is strong enough ($> k_B T$) and the adsorption sites are discrete. The exact nature of interaction between segments (as was observed with the two different segment–segment repulsion terms) will determine the value of Γ as well as σ^* . In general, the energies for such interactions are greater than $k_B T$, and this adsorption model could prove applicable.

Acknowledgment. This work was supported by the NSF and MRSEC under award numbers DMR-9400334 and DMR-9808941. C.J.B. acknowledges NSERC Canada for financial assistance, and the authors are grateful to Professors M. Olvera de la Cruz and A. C. Balazs for helpful discussions.

Appendix A: Loop Entropy

Consider N_2 unconstrained chains of length N on M_0 sites such that $NN_2 + N_1 = M_0$ where N_1 is the number of solvent molecules. The number of ways of putting the first monomer of the $(i + 1)$ th chain on any site is $(M_0 - Ni)$ and every successive one is $(M_0 - Ni)(c - 1)/M_0$ where c is the coordination number. The number of ways of putting all N monomers of the $(i + 1)$ th chain is²⁹

$$w_{i+1} \approx (M_0 - Ni)^N \left[\frac{(c - 1)}{M_0} \right]^{N-1} \quad (9)$$

and the number number of ways of putting N_2 chains is the product of the above.

For $N_2 N/n$ constrained loops of length n , the number of ways of putting the first monomer of the $(i + 1)$ th loop is $(\sigma A - j)$ where $\sigma A = N_2 N/n$ is the total number of available surface sticker sites, and A is the dimensionless area. The approximate number of ways of putting all the monomers of the $(i + 1)$ th constrained loop is³

$$w'_{i+1} \approx (\sigma A - j)(M_0 - ni)^{(n-1)} \left[\frac{(c - 1)}{M_0} \right]^{(n-1)} \quad (10)$$

The loss of entropy upon adding this constraint is then proportional to

$$\begin{aligned} & \ln \frac{1}{N_2!} \prod_{i=1}^{N_2 N/n} w' - \ln \frac{1}{N_2!} \prod_{i=1}^{N_2} w \\ & \approx \sigma A [\ln(\sigma A) - 1] - \frac{N_2 N}{n} (\ln M_0 - 1) + \frac{N_1}{n} \ln \phi_1 \\ & \approx \frac{N_2 N}{n} \ln \left(\frac{N_2 N}{n M_0} \right) + \frac{N_1}{n} \ln(1 - \phi) \end{aligned}$$

The total entropy decrease per chain is

$$\frac{\Delta S}{k N_2} = \frac{N}{n} \ln \left(\frac{\phi}{n} \right) + \frac{(1 - \phi) N}{\phi n} \ln(1 - \phi) \quad (11)$$

Since $n = (\phi H / \sigma a)$, the above equation can be rewritten

$$\frac{\Delta S}{k N_2} = \frac{\sigma N a}{\phi H} \ln \left(\frac{\sigma a}{H} \right) + \frac{(1 - \phi) \sigma N a}{\phi^2 H} \ln(1 - \phi) \quad (12)$$

Appendix B: Equilibrium Condition

In the above system, it is the total number of chains in the system that is fixed rather than the total adsorbed amount, i.e.

$$M = (1 - f_{\text{ad}})M + f_{\text{ad}}M \quad (13)$$

where f_{ad} is the fraction of adsorbed chains and M is the total number of chains. The total volume fraction of chains in the system is the sum of the adsorbed volume fraction ϕ_{ad} (not the volume fraction within the layer, ϕ), and the solution volume fraction ϕ_{sol}

$$\begin{aligned} \phi_{\text{tot}} &= \phi_{\text{ad}} + \phi_{\text{sol}} \\ &= \phi_{\text{tot}} [f_{\text{ad}} + (1 - f_{\text{ad}})] \end{aligned} \quad (14)$$

The adsorbed volume fraction is related to the volume fraction within the layer as

$$\phi_{\text{ad}} = \phi \frac{V_L}{V} \quad (15)$$

where V_L is the total volume of the adsorbed layer, and V is the total volume. The total free energy in the system per molecule is then

$$\begin{aligned} \frac{F_{\text{tot}}}{M} &= f_{\text{ad}} F_{\text{ad}} + (1 - f_{\text{ad}}) F_{\text{sol}} \\ &= \frac{\phi V_L}{\phi_{\text{tot}} V} F_{\text{ad}} + \frac{(\phi_{\text{tot}} V - \phi V_L)}{\phi_{\text{tot}} V} F_{\text{sol}} \end{aligned} \quad (16)$$

F_{ad} is the free energy of adsorption per chain and F_{sol} is the free energy of a chain in solution. Minimization of eq 16 yields

$$\frac{\phi_{\text{tot}} V}{M} \frac{\partial F_{\text{tot}}}{\partial \phi} = V_L F_{\text{ad}} + \phi V_L \frac{\partial F_{\text{ad}}}{\partial \phi} - V_L F_{\text{sol}} = 0 \quad (17)$$

$$\frac{\phi_{\text{tot}} V}{M} \frac{\partial F_{\text{tot}}}{\partial H} = \phi \frac{\partial V_L}{\partial H} F_{\text{ad}} + \phi V_L \frac{\partial F_{\text{ad}}}{\partial H} - \phi \frac{\partial V_L}{\partial H} F_{\text{sol}} = 0 \quad (18)$$

Since $V_L = H \times \text{total area}$, the equilibrium conditions are

$$F_{\text{ad}} + \phi \frac{\partial F_{\text{ad}}}{\partial \phi} - F_{\text{sol}} = 0 \quad (19)$$

$$F_{\text{ad}} + H \frac{\partial F_{\text{ad}}}{\partial H} - F_{\text{sol}} = 0 \quad (20)$$

As long as the chemical potential is the same throughout the system, i.e., $F_{\text{ad}} = F_{\text{sol}}$, the minimizations with respect to ϕ and H in the main body are valid.

References and Notes

- (1) Yoo, D.; Shiratori, S.; Rubner, M. F. *Macromolecules* **1998**, *31*, 4309.
- (2) Shiratori, S.; Rubner, M. F. *Macromolecules* **2000**, *33*, 4213.
- (3) Banerjee, P.; Irvine, D. J.; Mayes, A. M.; Griffith, L. G. *J. Biomed. Mater. Res.* **2000**, *50*, 331.
- (4) Israelachvili, J. In *Intermolecular and Surface Forces with Application to Colloidal and Biological Systems*; Academic Press: London, 1985.
- (5) Balazs, A. C.; Singh, C.; Zhulina, E. *Macromolecules* **1998**, *31*, 6369.
- (6) Decher, G. *Science* **1997**, *277*, 1232.
- (7) Decher, G.; Hong, J. D.; Schmitt, J. *Thin Solid Films* **1992**, *210*, 831. Ferreira, M.; Cheung, J.; Rubner, M. F. *Thin Solid Films* **1994**, *244*, 806.
- (8) Laschewsky, A.; Wischerhoff, E.; Kauranen, M.; Persoons, A. *Macromolecules* **1997**, *30*, 8304.
- (9) Böhmer, M. R.; Evers, O. A.; Scheutjens, J. M. H. M. *Macromolecules* **1990**, *23*, 2288.
- (10) Muthukumar, M. *J. Chem. Phys.* **1987**, *86*, 7230.
- (11) Scheutjens, J. M. H. M.; Fleer, G. J. *J. Phys. Chem.* **1980**, *84*, 178.
- (12) Israëls, R.; Leermakers, F. A. M.; Fleer, G. J. *Macromolecules* **1994**, *27*, 3087.
- (13) Shubin, V.; Linse, P. *Macromolecules* **1997**, *30*, 5944.
- (14) Vermeer, A. W. P.; Leermakers, F. A. M.; Koopal, L. K. *Langmuir* **1997**, *13*, 4413.
- (15) Netz, R. R.; Joanny, J.-F. *Macromolecules* **1999**, *32*, 9013.
- (16) Borukhov, I.; Andelman, D.; Orland, H. *Macromolecules* **1998**, *31*, 1655. Borukhov, I.; Andelman, D.; Orland, H. *J. Phys. Chem. B* **1999**, *103*, 5042.
- (17) Linse, P. *Macromolecules* **1996**, *29*, 326.
- (18) Van der Schee, H. A.; Lyklema, J. *J. Phys. Chem.* **1984**, *88*, 6661.
- (19) Yamakov, V.; Milchev, A.; Borisov, O.; Dünweg, B. *J. Phys.: Condens. Matter* **1999**, *11*, 9907.
- (20) Beltrán, S.; Hooper, H. H.; Blanch, H. W.; Prausnitz, J. M. *Macromolecules* **1991**, *24*, 3178.
- (21) Ellis, M.; Kong, C. Y.; Muthukumar, M. *J. Chem. Phys.* **2000**, *112*, 8723.
- (22) Balazs, A. C.; Huang, K.; McElwain, P. *Macromolecules* **1991**, *24*, 714. van der Linden, C. C.; van Lent, B.; Leermakers, F. A. M.; Fleer, G. J. *Macromolecules* **1994**, *27*, 1915.
- (23) Andelman, D.; Joanny, J.-F. *J. Phys. II Fr.* **1993**, *3*, 121.
- (24) See, for example the descriptions by: Aubouy, M.; Raphaël, E. *Macromolecules* **1998**, *31*, 4357. Manghi, M.; Aubouy, M. *Macromolecules* **2000**, *33*, 5721.
- (25) Holmes-Farley, S.; Bain, C.; Whitesides, G. M. *Langmuir* **1998**, *4*, 921.
- (26) Wasserman, S. R.; Tao, Y.-T.; Whitesides, G. M. *Langmuir* **1989**, *5*, 1074.
- (27) Marques, C. M.; Joanny, J.-F. *Macromolecules* **1990**, *23*, 268.
- (28) de Gennes, P.-G. *Macromolecules* **1980**, *13*, 1069.
- (29) Flory, P. J. *Principles of Polymer Chemistry*; Cornell University Press: Ithaca, NY, 1971.
- (30) de Gennes, P.-G. *J. Phys.* **1976**, *37*, 1445.
- (31) Daoud, M.; de Gennes, P.-G. *J. Phys.* **1977**, *38*, 85.
- (32) Alexander, S. *J. Phys.* **1977**, *38*, 983.
- (33) Cohen Stuart, M. A. *J. Phys. Fr.* **1988**, *49*, 1001.
- (34) Aguilera-Granja, F.; Kikuchi, R. *Physica A* **1992**, *189*, 81.
- (35) Sukhishvili, S. A.; Granick, S. *J. Chem. Phys.* **1998**, *109*, 6861.